

# DWT based Digital Watermarking Fidelity and Robustness Evaluation

Franco A. Del Colle\*      Juan Carlos Gómez

Laboratory for System Dynamics and Signal Processing

FCEIA, Universidad Nacional de Rosario

CIFASIS, CONICET

Riobamba 245 bis, 2000 Rosario, Argentina

{delcolle, jcgomez}@fceia.unr.edu.ar

## ABSTRACT

An Image Adaptive Watermarking method based on the Discrete Wavelet Transform is presented in this paper. The robustness and fidelity of the proposed method are evaluated and the method is compared to state-of-the-art watermarking techniques available in the literature. For the evaluation of watermark transparency, an image fidelity factor based on a perceptual distortion metric is introduced. On the other hand, a degradation factor is introduced for the evaluation of watermark robustness against JPEG compression and resizing. The new fidelity metric allows a perceptually aware objective quantification of image fidelity. The suitability of the proposed metric for the fidelity evaluation of still image watermarking is supported by simulation results.

**Keywords:** Digital Watermarking, Discrete Wavelet Transform, Perceptual Metrics.

## 1. INTRODUCTION

In the last decade, an important research effort has been devoted to the development of techniques addressing the issue of digital data protection. Among them, Digital Watermarking has become the most efficient and widely used.

Digital Watermarking refers to techniques that are used to protect digital data by imperceptibly embedding information (the watermark) into the original data in such a way that always remains present. As pointed out in [2], a set of requirements should be met by any watermarking technique. The main requirements are *perceptual transparency*, *payload of the watermark* and *robustness*. Perceptual transparency refers to the property of the watermark of being imperceptible in the sense that humans can not distinguish the watermarked images from the original ones by simple inspection. Payload of the watermark refers to the amount of information stored in the watermark, which in general depends on the application. Finally, robustness refers to the capacity of the watermark to remain detectable after alterations due to processing techniques or intentional attacks.

Good overviews on the state of the art of classical watermarking techniques can be found in the recent textbooks [2] and [7], and in [8], [10], [12] and the references therein.

Several techniques have been proposed in the literature for the watermarking of still images. From a general point of view, embedding is achieved by first extracting a set of features from the image to be watermarked, and then modifying them according to the watermark content. Thus, two

steps are required to define the embedding process: choice of the features to be modified, and definition of the embedding rule. Several solutions have been proposed, leading to different watermarking schemes. The different approaches can be classified taking into account different aspects. When the domain in which the watermark is being embedded is considered, a classification in spatial domain techniques and transform domain techniques can be made [8]. When the watermark adaptation to the particular image is considered, a classification in Image Adaptive Watermarking (IAW) methods ([3], [12], [13], [15]) and Image Independent Watermarking (IIW) methods ([6], [11]) can be done. In the IAW techniques the length, location and amplitude of the watermark are adapted to the image characteristics, while in the IIW techniques the length of the inserted watermark does not depend on the particular image. This paper will focus on Image Adaptive Discrete Wavelet Transform (IADWT) domain watermarking techniques since they have proved to yield better results regarding transparency and robustness.

Typically, the evaluation of the performance of a watermarking scheme is carried out by quantifying the perceptual transparency of the watermark and its robustness against several signal processing operations such as compression, scaling, cropping, etc. [13], [9].

Several image quality metrics have been used in the literature for the evaluation of watermark transparency, and can be classified into perceptual and non perceptual metrics depending on whether they take into account the characteristics of the Human Visual System (HVS) or not. Among the firsts, the Komparator metric in [1] and the Structural Similarity Index in [16] can be mentioned. On the other hand, the standard Root Mean Square Error (RMSE) or the Peak Signal-to-Noise Ratio (PSNR) are usually employed as non perceptual metrics. In [9], the authors perform watermark fidelity assessment for different watermarking schemes using the perceptual metrics in [1] and [16].

The evaluation of watermark robustness is typically performed by quantifying the capacity of the watermark to survive standard image processing operations. A thorough study of watermark robustness evaluation for different watermarking schemes can be found in [13].

In this paper, a new criterion (*fidelity factor*) for watermark transparency evaluation is proposed based on perceptual distortion metrics. The distortion metrics are based on a model of the Human Visual System that takes into account the different sensitivity of the human eye for color discrimination, contrast masking and texture masking. The proposed *fidelity factor* proves to have a better correlation with subjective evaluations than the standard Root

\*Author to whom all correspondence should be addressed.

Mean Square Error. In addition, a novel watermarking scheme in the DWT domain is proposed as a modification of the one in [13], which will prove to have a better performance, regarding transparency and robustness against JPEG-compression and re-scaling.

The rest of the paper is organized as follows. In section 2, the IADWT technique is briefly described. A slight variation of the IADWT method in [13] is also introduced in this section. In section 3, the perceptual metric used for the evaluation of the fidelity performance is described and a new *fidelity factor* is introduced also there. The robustness criterion to evaluate watermark detectability after attacks is described in section 4. Results on the comparison between the proposed method and the method in [13] during insertion and detection are presented in section 5. Finally, some concluding remarks are given in section 6.

**2. IMAGE ADAPTIVE DWT WATERMARKING**

Image adaptive watermarking methods make use of visual models in order to determine the maximum length and power of the watermark according to the image capacity to "hide information" without being perceptible. This capacity is calculated by means of the so called Just Noticeable Differences (JND) thresholds, which measure the smallest difference between images which is perceptually detectable by the human eye. In the DWT domain, these thresholds allows to determine the location of the transform coefficients and the amount that they can vary without being noticeable in the spatial domain.

In the watermark embedding scheme in [13], the watermark is modulated by the JND, and the coefficients are marked whenever they are greater than the JND threshold, *i.e.*

$$\hat{X}^w(u, v) = \begin{cases} \hat{X}(u, v) + J(u, v)w(\ell) & \hat{X}(u, v) > J(u, v) \\ \hat{X}(u, v) & \text{otherwise} \end{cases} \quad (1)$$

where  $\hat{X}(u, v)$  and  $\hat{X}^w(u, v)$  are the DWT coefficients of the original image and the watermarked image respectively, and  $J(u, v)$  is the JND matrix at the  $u, v$  frequency in the DWT domain.

In this scheme, the watermark sequence  $w(\ell)$  is generated from a zero mean, unit variance, normally distributed random sequence. In this way, the watermark sequence weighted by the JND thresholds has lower power than the maximum power that can be inserted without causing noticeable distortions in the image. Figure 1 schematically depicts the image adaptive watermarking embedding scheme, where  $X(i, j)$  denotes the original image and  $X^w(i, j)$ , the watermarked image.

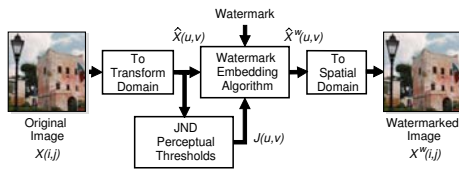


Figure 1: Image Adaptive Watermarking Embedding Scheme.

The JND thresholds are computed based on a perceptual model of the Human Visual System (HVS). A widely used perceptual model is the one introduced by Watson in [17]. This model takes into account frequency sensitivity, local luminance and contrast masking effects to

determine an image-dependent quantization matrix, which provides the maximum possible quantization error in the DWT coefficients which is not perceptible by the HVS. This model has been used by the image compression standard JPEG2000 [14], where the JND thresholds determine the optimal quantization step sizes or bit allocations for different parts of the image to be compressed.

In the watermark detection scheme the JND are calculated using the original image, then, the DWT coefficients of the original image are subtracted from the ones of the image suspected to be watermarked, and this difference is divided by the JND in order to obtain the received watermark. The correlation between the extracted watermark and the original one is then performed and the maximum value is determined, *i.e.*

$$w_e(\ell) = \frac{\hat{X}^w(u, v) - \hat{X}(u, v)}{J(u, v)} \quad \text{if } \hat{X}(u, v) > J(u, v) \quad (2)$$

$$r_{w, w_e} = \frac{w_e(\ell) * w(-\ell)}{E_{w_e} \cdot E_w} \quad (3)$$

where  $E_{w_e}$  and  $E_w$  are the energies of the extracted watermark sequence,  $w_e(\ell)$ , and the original watermark sequence,  $w(\ell)$ , respectively. Figure 2 schematically depicts the image adaptive watermarking detection scheme.

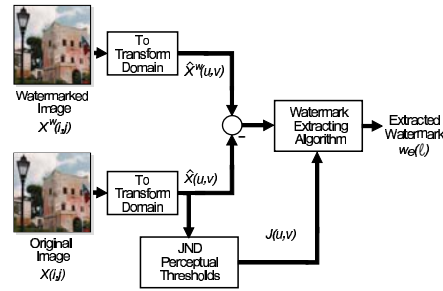


Figure 2: Image Adaptive Watermarking Detection Scheme.

The IADWT method has been studied in [13] and the authors pointed out two main advantages with respect to the IIV methods. First, non adaptive watermarking techniques are less robust, in order to guarantee transparency for a wide variety of input images. This is in contrast to the image adaptive approach which allows the watermark signal to reach the perceptual upper limit given by the JND thresholds. Second, for images with large uniform areas, heuristic techniques based on a global transform (like the one in [6]), could result in visible watermarks since the algorithms are not able to adapt to local image characteristics. On the other hand, the JND paradigm adapts the watermark not only to the global characteristics associated to the viewing conditions, but also to the local image characteristics associated with visual masking effects.

The following modification to the IADWT insertion scheme in Eq. (1) can be introduced

$$\hat{X}^w(u, v) = \begin{cases} \hat{X}(u, v) + J(u, v)w(\ell) & \hat{X}(u, v) > J(u, v) > T \\ \hat{X}(u, v) & \text{otherwise} \end{cases} \quad (4)$$

This modified insertion scheme will be hereafter denoted as IADWT<sub>T</sub>. The *rationale* for the constrain  $J(u, v) > T$  is that when the JND thresholds are too small, the magnitude of the marking term in Eq. (4) becomes negligible. The introduction of the lower bound  $T$  has then the advantage

of reducing the watermark length, improving in this way the fidelity and also the robustness, as will be illustrated in section 5.

The detection scheme in Eq. (2) has to be modified to take into account the modification in the insertion scheme, as follows

$$w_e(\ell) = \frac{\widehat{X}^w(u,v) - \widehat{X}(u,v)}{J(u,v)} \quad \text{if } \widehat{X}(u,v) > J(u,v) > T \quad (5)$$

### 3. FIDELITY EVALUATION USING PERCEPTUAL METRICS

In the evaluation of image watermarking methods it may be of interest to judge the fidelity of the inserted watermark. Basically the fidelity is a measure of the similarity between the images before and after the watermark insertion. For some watermarking applications, fidelity is the primary perceptual measure of concern, thus the watermarked image must be indistinguishable from the original.

In studies that involve the judgment by human beings, it is important to recognize that visual sensitivity can vary significantly from individual to individual, and moreover that sensitivity can change over time in any one individual. Therefore, it is common that studies involving human evaluation use a large number of subjects and perform a large number of trials, resulting in experiments that are statistical in nature and which become expensive and time consuming if a large group is being considered. To avoid the dependence on human judgement it would be desirable to objectively quantify the fidelity of watermarked images based on a metric that takes into account the characteristics of the HVS.

Image fidelity metrics appeared in the context of imaging applications to quantify the distortion in images produced by processing algorithms such as compression, halftoning, printing, etc. Different metrics have been proposed in the literature to measure image distortion (see [18] for a thorough treatment of distortion metrics and the more recent work [16]). Among them, the ones based on the characteristics of the HVS have proved to deliver the best results, since they take into account the different sensitivity of the human eye for color discrimination, contrast masking and texture masking.

A metric widely used to measure fidelity is the CIELAB metric [4] that specifies how to transform physical image measurements into perceptual differences ( $\Delta E$ ). The metric was derived from perceptual measurements of color discrimination of large uniform targets. A modification of the  $\Delta E$  formula was released by CIE (International Commission on Illumination, Vienna) in 1994 based on new experimental data. The new formula was found to predict color differences slightly better than the old formula and it was named CIE94 [5].

An extension of CIELAB, named S-CIELAB [20], includes the spatial-color sensitivity of the human eye. The S-CIELAB metric incorporates the different spatial sensitivities of the three opponent color channels by adding a spatial pre-processing step before the standard CIELAB  $\Delta E$  calculation. The S-CIELAB metric achieves this by removing the image components that cannot be seen by the naked eye. S-CIELAB consists of three processing steps. First, the original and distorted images, which are represented in a device-dependent space, are converted into a device-independent representation consisting of one luminance and two chrominance color components for each image, known as the YCbCr color space. Second, each component im-



Figure 3: Left: Original Image. Center: Noisy Image. Right: Distortion Map.

age is passed through a spatial filter that is selected according to the spatial sensitivity of the human eye for that color component. Third, the filtered images are transformed into the CIE*Lab* color space format such that the color difference formula can be applied to give a S-CIELAB  $\Delta E_{94}$  map, which indicates where the visible distortions are in the image, and how large the distortions are.

In [19] the authors test how well the S-CIELAB metric predicts image fidelity for a set of color images by comparison with two other metrics, namely, the widely used root mean square error (point-by-point RMS) computed in un-calibrated RGB values and the point-by-point CIELAB  $\Delta E_{94}$  values.

Since the S-CIELAB metric takes into account the perceptual characteristics of the HVS, such as color discrimination, different spatial sensitivity, etc., this metric represents a natural choice for the quantification, in an objective way, of the fidelity of watermarked images. To the best of the authors' knowledge, this perceptual evaluation of the fidelity based on the S-CIELAB metric has not been considered before in the context of Color Images Digital Watermarking.

To illustrate the use of the S-CIELAB metric, a region of the left image in Figure 3, delimited by the white square in the center image, is corrupted with zero mean unit variance additive Gaussian white noise. The right image shows the image distortion map corresponding to the noise corrupted image, where the S-CIELAB  $\Delta E_{94}$  values are shown with a grayscale color map. The pixels where the S-CIELAB  $\Delta E_{94}$  values are above a specified threshold are then marked in green. For reference purposes the edges of the original image are displayed in white. Note the reader that there are no perceptible differences between the original and corrupted images (left and center images in Figure 3, respectively).

The idea in this paper is to use distortion maps to compare watermarked image fidelity for the two insertion methods described in section 2. Due to the spatial distribution of the S-CIELAB  $\Delta E_{94}$  errors in the distortion maps (the green marks in the right image of Figure 3) it is difficult to make a comparison of the different methods. To provide a unique parameter quantifying this fidelity, a pooling of the S-CIELAB  $\Delta E_{94}$  errors is proposed as follows:

$$\mathcal{F} \triangleq \left( 1 - \frac{\sum_{i=1}^M \sum_{j=1}^N (S\Delta E_{94}(i,j)Mask(i,j))}{\sum_{i=1}^M \sum_{j=1}^N \sqrt{X_L(i,j)^2 + X_a(i,j)^2 + X_b(i,j)^2}} \right) \times 100 \quad (6)$$

where  $S\Delta E_{94}$  is a matrix with the values of the S-CIELAB  $\Delta E_{94}$  errors for each pixel, *i.e.* the image distortion map,  $Mask$  is a mask with ones in the positions where the S-CIELAB  $\Delta E_{94}$  errors are above the threshold and zeros otherwise,  $X_L$ ,  $X_a$  and  $X_b$  are the image components in the *Lab* color space. Values of  $\mathcal{F}$  close to 100 % indicate that no perceptible distortion is present in the watermarked image.

The performance of the proposed metric will be compared in section 5 with that of a standard non perceptual metric based on the Root Mean Square (RMS) error. This metric, namely RMS Fit ( $RMS_{FIT}$ ), is obtained by making

a pooling of the RMS errors, resulting in:

$$RMS_{FIT} \triangleq \left( 1 - \frac{\sum_{i=1}^M \sum_{j=1}^N \sqrt{\Delta X_R(i,j)^2 + \Delta X_G(i,j)^2 + \Delta X_B(i,j)^2}}{\sum_{i=1}^M \sum_{j=1}^N \sqrt{X_R(i,j)^2 + X_G(i,j)^2 + X_B(i,j)^2}} \right) \times 100 \quad (7)$$

where the subindexes  $R$ ,  $G$  and  $B$  denote the corresponding image components in the RGB color space.

#### 4. ROBUSTNESS EVALUATION

Another important issue when evaluating image watermarking methods is the robustness, *i.e.*, the capacity of the watermark to survive standard image processing alterations, such as lossy compression, scaling, cropping, printing and scanning, etc..

In this paper, robustness of the watermark against JPEG compression and re-scaling is evaluated by computing a degradation coefficient,  $D$ , which quantifies the degradation in the watermark detectability caused by these image processing tasks. To perform the robustness test, the watermarked image is subjected to each one of the above mentioned attacks, and then the watermark is extracted following the procedure described in section 2. The normalized cross-correlation between the original and the extracted watermarks is then computed. The *detectability degradation coefficient* is then defined as,

$$D \triangleq (1 - r_{w,w_e}(0)) \times 100 \quad (8)$$

where  $r_{w,w_e}(k) \triangleq r_{w,w_e}(k)|_{k=0}$  denotes the normalized correlation between the original watermark,  $w(\ell)$ , and the extracted watermark,  $w_e(\ell)$ , at lag  $k = 0$ .

#### 5. RESULTS

In order to compare the performance of the proposed watermarking scheme IADWT<sub>T</sub> and the IADWT in [13], a set of (256 × 256) natural color images was used. To make the results independent of the particular set of natural images considered, the same tests were also performed on synthetic pattern images with large uniform areas (like Image 4 in Figure 4.D) and images with predominant high frequency regions (like Image 5 in Figure 4.E).

Due to space limitations the results corresponding to only five images are presented in this paper. The original images, called Image 1 to Image 5, are shown in Figure 4.

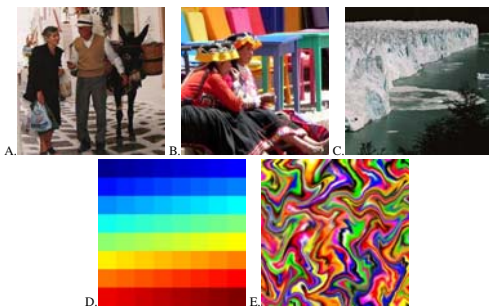


Figure 4: A. Image 1, B. Image 2, C. Image 3, D. Image 4 and E. Image 5.

##### Fidelity Evaluation results

In this section two separate tests to evaluate fidelity will be performed. The purpose of Test 1 in subsection 5 is to illustrate the fact that the fidelity factor  $\mathcal{F}$  defined in Eq. (6) provides a much better assessment of image quality than the

standard  $RMS_{FIT}$ . On the other hand, Test 2 in subsection 5 is designed to compare the fidelity of the two DWT based insertion schemes described in Section 2.

**Fidelity Test 1** In order to illustrate the fact that the  $RMS_{FIT}$  does not provide an objective assessment of image quality, a watermarked image with a strong watermark was generated with the IIW embedding technique proposed in [6]. In this method, the watermark, denoted  $\{w(\ell)\}_{\ell=1}^L$ , is a length  $L$  sequence of normally distributed, zero-mean unit-variance random numbers. Let  $X(i, j)$  be the original image,  $X^w(i, j)$  the watermarked image, and  $\hat{X}(u, v)$  and  $\hat{X}^w(u, v)$  their corresponding DCT coefficients. The embedding algorithm in [6] takes the  $L$  most significant non-DC DCT coefficients and marks them as follows:

$$\hat{X}_\ell^w(u, v) = \hat{X}_\ell(u, v)(1 + \alpha w(\ell)) \quad (9)$$

where  $\alpha$  is a scale factor which prevents unreasonable values for  $\hat{X}_\ell^w(u, v)$ . The authors propose an empirically determined value of 0.1 for  $\alpha$  and they choose to insert the watermark in the 1000 most significant non-DC DCT coefficients. After the watermark is embedded, the watermarked image  $X^w(i, j)$  is obtained by inverse transforming all the DCT coefficients.

The original and the marked images are shown in the left and right sides of Figure 5, respectively. In this case the  $\alpha$  parameter was chosen equal to 0.25, resulting in a fidelity factor  $\mathcal{F} = 34.04\%$  and a  $RMS_{FIT} = 91.26\%$ . Based only on the  $RMS_{FIT}$  one would expect no noticeable distortions on the watermarked image which is not the case for this example (particularly in the sky portion at the top of the image). The fidelity factor  $\mathcal{F}$  in turn gives a better assessment of image quality.



Figure 5: Left: Original Image. Right: Watermarked Image.

**Fidelity Test 2** The values of the watermark length  $L$ , the normalized watermark energy in the spatial domain  $E$  (or equivalently, the normalized mean square error between the original and the watermarked images), the fidelity factor  $\mathcal{F}$ , and the  $RMS_{FIT}$  were computed for the five images in Figure 4, marked using the IADWT and IADWT<sub>T</sub> insertion schemes described in Section 2. The results are shown in Table 1.

As can be observed from the fifth column in Table 1 there is no noticeable difference between the fidelity, as measured by the  $RMS_{FIT}$ , using both insertion schemes. The difference is more noticeable using the proposed fidelity factor, as can be observed from the values in the fourth column.

The values of the fidelity factor,  $\mathcal{F}$ , in Table 1 show that the IADWT<sub>T</sub> method consistently outperforms the IADWT method regarding fidelity. Even for the case of images with large uniform color regions, as the one in Figure 4.D, where the image adaptive methods are supposed to work poorly

Table 1: Experimental results on Fidelity Evaluation for Images 1 to 5.

	$L$	$E$ ( $\times 10^{-3}$ )	$\mathcal{F}$ (%)	$RMS_{FIT}$ (%)
Image 1				
IADWT	8347	1.40	82.55	97.45
IADWT <sub>T</sub>	874	0.38	95.16	99.20
Image 2				
IADWT	9314	1.26	84.42	97.52
IADWT <sub>T</sub>	1036	0.37	95.55	99.22
Image 3				
IADWT	8196	1.76	79.68	97.11
IADWT <sub>T</sub>	1117	0.65	94.18	98.90
Image 4				
IADWT	3002	0.12	97.81	99.17
IADWT <sub>T</sub>	1138	0.07	99.21	99.67
Image 5				
IADWT	11336	1.06	89.01	97.56
IADWT <sub>T</sub>	1458	0.33	95.44	99.05

[13], the IADWT<sub>T</sub> method produces non perceptible watermarks. On the other hand, the IADWT method produces visible distortions, as can be observed from Figure 6 (see for instance the spots in the green regions of the upper left image).

The left columns in Figures 6 and 7 show the watermarked images corresponding to Image 1 and Image 4 using the above mentioned watermarking schemes (namely IADWT and IADWT<sub>T</sub> from top to bottom). The right columns show the corresponding distortion maps obtained after applying the S-CIELAB  $\Delta E_{94}$  metric to the watermarked images. As expected, the distortion is larger in the regions with high frequency components, resulting in a less perceptible watermark due to the masking phenomenon of the HVS.

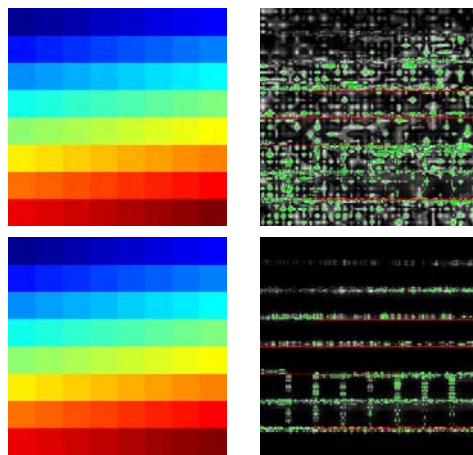


Figure 6: Left Column: Watermarked Image 4 using IADWT (top) and IADWT<sub>T</sub> (bottom). Right Column: Corresponding distortion maps.

**Robustness Evaluation Results**

In this subsection the robustness of the watermarked images against JPEG compression and re-scaling is evaluated, for both image adaptive DWT-based watermarking schemes.

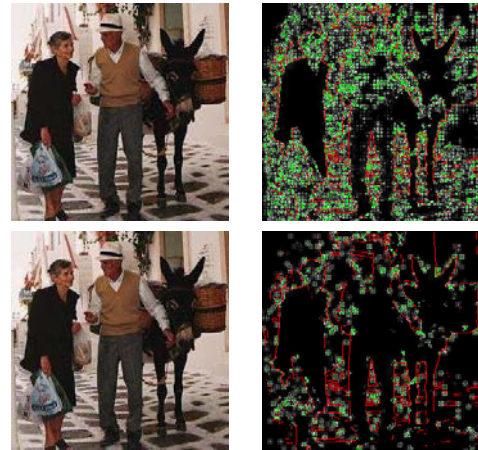


Figure 7: Left Column: Watermarked Image 1 using IADWT (top) and IADWT<sub>T</sub> (bottom). Right Column: Corresponding distortion maps.

**JPEG Compression** The detectability degradation coefficient  $\mathcal{D}$ , as defined in Eq. (8), is computed for both image adaptive DWT-based watermarking schemes when JPEG-compression with quality factors in the range [95%-75%] is applied. The results for Images 1, 4 and 5 are shown in Figure 8 from top to bottom respectively. As can be observed the IADWT<sub>T</sub> watermarking scheme consistently outperforms the IADWT one regarding robustness against this image processing operation.

**Re-scaling** The robustness against re-scaling is tested by first resizing the watermarked image to half of its size and then enlarging the image to its original size. Both image resizing operations are performed using the nearest neighbor interpolation method. The detectability degradation coefficient  $\mathcal{D}$  is then computed for both image adaptive DWT-based watermarking schemes. The results are shown in Table 2. It can be observed that the IADWT<sub>T</sub> scheme outperforms the IADWT one for most of the images, the exception being for Image 4 which has large uniform color regions. Results not shown in Table 2 suggest that this behavior applies for images with large uniform color regions in general.

Table 2: Detectability degradation coefficient for 50% re-scaling.

	Scaling (50%)				
	Im. 1	Im. 2	Im. 3	Im. 4	Im. 5
IADWT	89.11	89.13	89.70	29.37	85.63
IADWT <sub>T</sub>	54.63	62.92	63.28	42.95	51.25

**6. CONCLUDING REMARKS**

An image fidelity factor based on the S-CIELAB  $\Delta E_{94}$  perceptual distortion metric has been introduced in this paper for the purposes of evaluating the distortion introduced by different IADWT watermark insertion algorithms. The use of this metric allows a perceptually aware objective quantification of image fidelity. Simulation results show the suitability of the proposed metric in the framework of

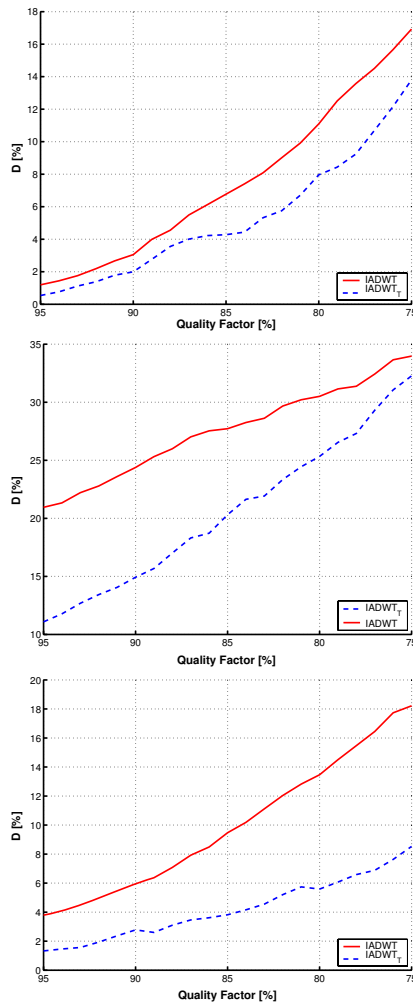


Figure 8: From Top to Bottom: Detectability degradation coefficient vs. JPEG Quality Factor for Images 1, 4 and 5, for IADWT and IADWT<sub>T</sub> watermarking schemes.

still image digital watermarking. In addition, a new IADWT watermarking scheme has been introduced. The robustness against compression and re-scaling, and the fidelity of the proposed method have been investigated and the results show that the proposed technique outperforms other methods available in the literature. A work is in progress where the proposed *fidelity factor* is being validated through subjective tests. Preliminary results show a good correlation of the proposed metric with the subjective assessment.

7. REFERENCES

[1] D. Barba and P. Le Callet. A robust quality metric for color image quality assesment. In *Proc. of the IEEE International Conference on Image Processing*, pages 437–440, 2003.

[2] M. Barni and F. Bartolini. *Watermarking Systems Engineering - Enabling Digital Assets and Other Applications*. Marcel Dekker, Inc., New York, 2004.

[3] M. Barni, F. Bartolini, and A. Piva. Improved wavelet-based watermarking through pixel-wise masking. *IEEE Transactions on Image Processing*, 10(5):783–791, May 2001.

[4] CIE: International Commission on Illumination. Rec-

ommendations on uniform color spaces, color difference equations, psychometrics color terms. Technical Report CIE 15 (E.-1.3.1), Supplement No.2, Vienna, Austria, 1971.

[5] CIE: International Commission on Illumination. Industrial colour-difference evaluation. Technical Report CIE 116-95, Austria, 1995.

[6] I. Cox, J. Kilian, F. Leighton, and T. Shamoan. Secure spread spectrum watermarking for multimedia. *IEEE Transactions on Image Processing*, 6(12):1673–1687, December 1997.

[7] I. Cox, M. Miller, and J. Bloom. *Digital Watermarking*. Morgan Kaufmann, San Francisco, 2002.

[8] G. Langelaar, I. Setyawan, and R. Lagendijk. Watermarking digital image and video data. *IEEE Signal Processing Magazine*, 17(5):20–46, 2000.

[9] E. Marini, F. Autrusseau, P. Le Callet, and P. Campisi. Evaluation of standard watermarking techniques. In *Security, Steganography, and Watermarking of Multimedia Contents IX, Proc. of SPIE-IS& Electronic Imaging*, volume 6505, pages 1–10, San Jose, CA, USA, 2007.

[10] F. Petitcolas. Watermarking schemes evaluation. *IEEE Signal Processing Magazine*, 17(5):58–64, September 2000.

[11] A. Piva, M. Barni, E. Bartolini, and V. Cappellini. DCT-based watermark recovering without resorting to the uncorrupted original image. In *Proceedings of the International Conference on Image Processing*, volume 1, pages 520–523, 1997.

[12] C. Podilchuk and E. Delp. Digital watermarking: Algorithms and applications. *IEEE Signal Processing Magazine*, 18(4):33–46, July 2001.

[13] C. Podilchuk and W. Zeng. Image-adaptive watermarking using visual models. *IEEE Journal on Selected Areas in Communications*, 16(4):525–539, May 1998.

[14] A. Skodras, C. Christopoulos, and T. Ebrahimi. The JPEG 2000 still image compression standard. *IEEE Signal Processing Magazine*, 18(5):36–58, Sept. 2001.

[15] M. Swanson, B. Zhu, and A. Tewfilc. Transparent robust image watermarking. In *Proceedings International Conference on Image Processing*, volume 3, pages 211–214, 1996.

[16] Z. Wang, A.C. Bovik, H.R. Sheikh, and P.E. Simoncelli. Image quality assessment: from error visibility to structural similarity. *IEEE Transactions on Image Processing*, 13(4):600–612, 2004.

[17] A. Watson, G. Yang, J. Solomon, and J. Villasenor. Visibility of wavelet quantization noise. 6(8):1164–1175, August 1997.

[18] S. Winkler. *Digital Video Quality Vision Models and Metrics*. John Wiley & Sons Ltd, Chichester, UK, 2005.

[19] X. Zhang and B. Wandell. Color image fidelity metrics evaluated using image distortion maps. *Signal Processing*, 70:201–214, 1998.

[20] Z. Zhang. A spatial extension to CIELAB for digital color image reproduction. *Society for Information Display Symposium Technical Digest*, 27:731–734, 1996.